Measuring the Lifetime of Cosmic-Ray Muons

Thomas Malthouse MS 560
Reed College

Muons are unstable, electron-like particles formed in collisions between cosmic rays and the upper layers of the atmosphere, with a lifetime of about (2197.03 ± 0.04) ns in free space and (2117 ± 3) ns in plastic. We can observe these muons as they pass through a plastic scintillation detector, and again if they happen to decay in the detector. We observed 1125 of these decays, and estimated the probability density function underlying their times. By fitting an exponential distribution to these observations, we estimated a lifetime of (2058 ± 86) ns—an error of 0.68σ from the accepted value.

I. INTRODUCTION

The muon is an elementary particle, and behaves much like an unstable, heavier electron. Under the standard model of particle physics (see Fig. 1), it is classified as a lepton, with a spin of 1/2 and a charge of e, but with a rest mass energy about 200 times larger than the electron's. Created in high-energy collisions (most commonly, when cosmic rays hit the Earth's atmosphere), they have a mean lifetime of approximately 2 µs before decaying as follows: [1]

$$\begin{aligned} \mu^- &\to e^- + \bar{\nu_e} + \nu_\mu \\ \mu^+ &\to e^+ + \nu_e + \bar{\nu_\mu} \end{aligned} \tag{1}$$

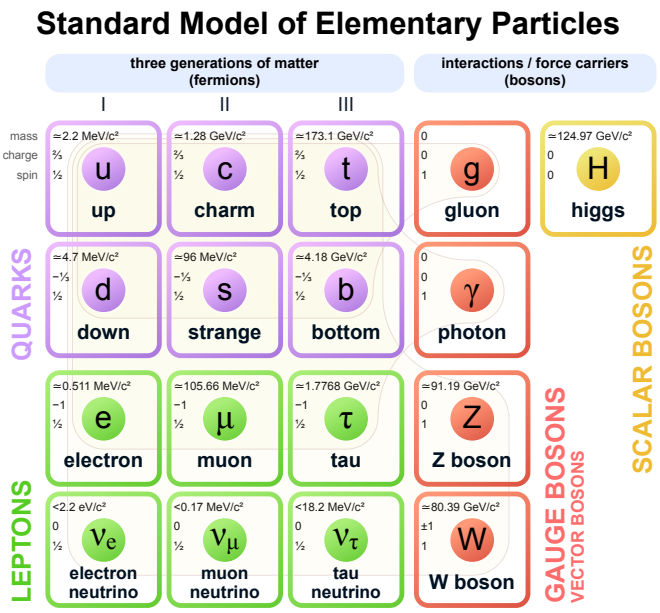

FIG. 1: The particles of the standard model of particle physics

Muons were first observed in 1936 by Carl Anderson and Seth Neddermayer, who discovered a particle with an unknown curve radius in a magnetic field while studying cosmic radiation and its byproducts [2]. The next year, J.C. Street and E.C. Stevenson confirmed the muon's existence and provided the first estimate of its mass, observing the track of muons passing through a cloud chamber and measuring their radius of curvature [3].

In matter, muons behave much like free electrons (more commonly known as beta particles). When a muon passes close to an atomic nucleus, the electric force on the muon induces an acceleration, although significantly lower than that of an electron (due to the muon's higher mass). This acceleration causes the muon to emit electromagnetic radiation, converting some of the muon's kinetic energy into light, which can then be detected and counted—a process known as *bremsstrahlung*, from the German for "braking radiation" [4].

When decaying, muons also release a free electron or positron—particles that interact with normal matter far more readily. Muon decays can therefore be detected by looking for high-energy beta particles, which are easily measured. By measuring the times between the initial detection of muons and their decay, we can estimate the distribution of muon lifetimes and the mean lifetime τ.

II. THEORY

A. Muon Sources

The Earth is constantly being bombarded by cosmic radiation. This radiation—originating largely from extrasolar sources—reflects the breakdown of matter in the universe, with approximately 70% of the radiation being free protons, and most of the the remainder being free electrons and alpha particles ($^4_2$He nuclei). Other elements created in stellar nucleosynthesis (carbon, oxygen, and iron, among others) also appear, as well as antiprotons and positrons [1].

These particles have been accelerated to relativistic velocities in violent astronomical events, including supernovae, galactic nuclei, and the merger of neutron stars [5] (although the exact source and nature of cosmic radiation is not yet entirely understood [6]). Once reaching the solar system, the solar wind shapes the flux of particles, strongly affecting the incidence of cosmic rays on Earth; as well as creating new particles (most notably, antiprotons and positrons) in solar wind-cosmic ray interactions—these new particles are known as *secondary cosmic radiation* [7].

When these energetic particles encounter the Earth's

atmosphere, they collide with the atoms of the atmosphere, causing a cascading chain reaction, forming exotic particles not found at lower energies—a phenomenon known as an *air shower*. One of the particles created in these reactions is the pion, a highly unstable combination of a quark and antiquark. After a mean lifetime of 26 ns, they decay through the weak force into a muon and muon neutrino:

$$\pi^+ \to \mu^+ + \nu_\mu$$
$$\pi^- \to \mu^- + \bar{\nu_\mu}$$

1. Muon Decay

As mentioned in the introduction, muons are unstable and decay into electrons and neutrinos. This decay, like all other radioactive decays, is probabilistic and governed by the differential equation

$$\frac{dN}{dt} = -\lambda N$$

such that the number of decays per second is given by the total population of muons times some decay constant λ. This equation has solution

$$N = N_0 e^{-\lambda t} = N_0 e^{-t/\tau}$$

where $\tau = 1/\lambda$ is the mean lifetime of the muon. Roughly speaking, given a population of muons, roughly $1/\tau$ of them will decay in a unit time. Note that the lifetime is completely independent of the population size, and so the equation is unaffected by time offsets:

$$N(t_0 + t) \propto e^{-\lambda(t_0+t)} = e^{-\lambda t_0} e^{-\lambda t} \propto e^{-\lambda t}$$

This means we do not have to worry about the time offset between muon creation and our measuring them when we determine τ.

2. Observing Length Contraction with Muons

As mentioned in the introduction, muons are highly unstable, with a time constant of about 2.2 µs. Even at ultrarelativistic velocities, the mean distance traveled before decay is

$$\log 2(2.2\,\mu\text{s}) \cdot (0.9997c) \approx 456\,\text{m}.$$

Since muons are created tens of kilometers above the surface of the Earth, the probability of a muon surviving long enough to reach the surface is absolutely minuscule. If we assume that a muon is created at a height of 30 kilometers, the probability of it reaching the surface is

$$P = e^{\frac{30\,\text{km}}{(0.9997c)2.2\,\mu\text{s}}} \approx 1.73 \times 10^{-20}$$

With a flux of approximately $10\,000\,\text{m}^{-2}\,\text{min}^{-1}$ [8], we know that our classical calculation for the mean distance must be incorrect. If we calculate the apparent distance to the ground in the muon's frame, we get that

$$L = L_0\gamma = 30\,\text{km}\sqrt{1 - 0.9997^2} = 735\,\text{m}$$

which allows a large proportion of muons to survive to the surface of the Earth. The muon flux on Earth's surface, combined with a measurement of its lifetime, is one of the most readily apparent demonstrations of special relativity.

B. Detector Physics

As discussed in §II A, muons in matter behave much like heavy electrons, converting kinetic energy to electromagnetic radiation as they travel. This electromagnetic radiation can then be detected using a variety of instruments, including gas-filled tubes, scintillators, and gamma spectrometers, each of which have inherent advantages and disadvantages in speed, sensitivity, cost, and discernability[1]. For our purposes, a plastic scintillator (with its quick response curve and robust solid-state construction) provides optimum performance [9].

A scintillator is a material that re-emits the energy deposited as light, which can then be measured by a photodetector or photomultiplier tube. Typically, these materials consist of a mixture of some substrate (which can be virtually any material that absorbs radiation, including glass, plastic, and even some liquids), and a fluorophore, which releases lower-frequency photons upon being excited by the x-rays released by bremsstrahlung [10].

In practice, scintillators often use more than one fluor to convert the x-ray into a detectable photon in the visible range [11]. Figure 2 visualizes this process, including the relative concentrations of each fluor. Note that only a small proportion of the energy of the incident photon is actually converted to visible photons and detected—the vast majority of the energy (over 95% for most scintillators) is used to excite the lattice structure of the crystal, slightly raising its temperature. Chapter 2 of Neal Woo's thesis ([11]) includes a very detailed treatment of scintillator physics, including energy dependence and the exact mechanism by which particles are slowed.

A decay event will only produce a few photons, so we need some way to amplify the signal into something that can easily be distinguished from electronic noise. A photomultiplier consists of a photocathode and anode, with a series of dynodes at increasing potentials in between the two (fig. 3). An incident photon hits the initial photocathode, releasing an electron. This electron then

[1] The ability to measure the energy of incident radiation.

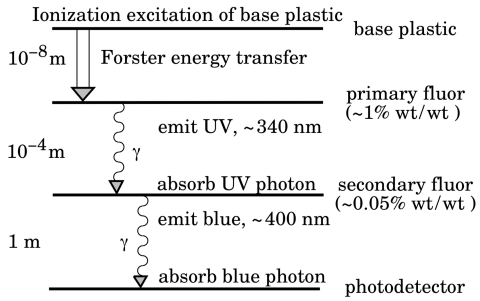

FIG. 2: The process of converting a high-energy x-ray photon into detectable blue photons using multiple fluors, including mean energy transfer distance and wavelengths. Figure from [1].

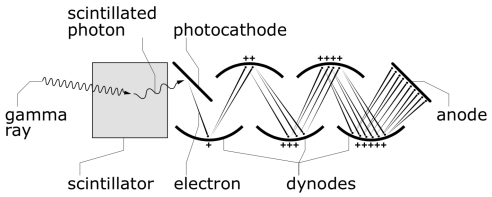

FIG. 3: The elements of a photomultiplier tube. Figure from [9].

accelerates to the first dynode, where its additional energy allows it to free multiple electrons. These electrons then repeat the process on the next dynode, turning a single incident photon into a flood [9].

C. Muons in Matter

1. Nuclear Absorption

So far, we have only considered muons being destroyed through decay into an electron (or positron) and a pair of neutrinos, as described in equation 1. However, negative muons (μ^-) can also become bound to a nucleus, much like an electron. Because the quantum states of muons are distinct from those of electrons, the Pauli Exclusion Principle does not apply, and the muons can occupy any orbital. Then, in a process analogous to electron capture, the muon can interact with a proton in the nucleus

$$\mu^- + \mathrm{p} \rightarrow \mathrm{n} + \nu_\mu + \gamma \tag{2}$$

before it naturally decays. Because negative muons have this additional destruction path, their mean lifetime in matter will be shorter than the free space value of $(2.197\,03 \pm 0.000\,04)\,\mu\mathrm{s}$. The difference in lifetimes heavily depends on the material, and scales approximately with Z^4—in Beryllium ($Z = 4$), the lifetime is around 2.1 µs, while it is as small as 20 ns in uranium [12]. If we treat the scintillator plastic as being made of pure carbon (a reasonable assumption, since this effect very rarely happens with hydrogen), we get an adjusted lifetime for negative muons of [13]

$$\tau^- \approx (2.043 \pm 0.003)\,\mu\mathrm{s}. \tag{3}$$

2. Observed Lifetime

Positive muons cannot undergo this process, so their lifetime in the scintillator will be identical to their lifetime in free space, and we can set $\tau^+ = \tau$. Since positive and negative muons have different decay times, the lifetime we will be able to measure for muons will depend on the ratio $\rho = N^+/N^-$. If we estimate $\rho = 1$, we can calculate the expected overall decay time to be

$$\begin{aligned}\tau_{\mathrm{obs}} &= (1+\rho)\frac{\tau^-\tau^+}{\tau^+ + \rho\tau^-} \\ &= 2\frac{\tau^-\tau^+}{\tau^+ + \tau^-} \\ &\approx (2.117 \pm 0.003)\,\mathrm{us}\end{aligned} \tag{4}$$

We expect ρ to be somewhat larger than 1, since some negative muons will be absorbed in the atmosphere, but still relatively close to 1, so this is a decent estimate. Alternatively, we can rearrange this equation to calculate the fraction of negative muons given our measured lifetime:

$$\rho = -\frac{\tau^+}{\tau^-}\left(\frac{\tau^-\tau_{\mathrm{obs}}}{\tau^+ - \tau_{\mathrm{obs}}}\right) \tag{5}$$

III. EXPERIMENTAL DESIGN & PROCEDURES

A. The Experiment

The detector is constantly being bombarded by muons—remember, the flux is around $10\,000\,\mathrm{m}^{-2}\,\mathrm{min}$ at seal level. As these muons pass through the chamber, they leave a trail of energy in their wake, as they are slowed by bremsstrahlung. Most pass through the detector, showing up as just a single peak. However, some are brought to a halt in the scintillator, and simply sit stationary before decaying. By measuring the times between muon entrance and decay on these double-peak events, we can estimate the probability density function (PDF) for muon lifetime, and therefore the lifetime τ.

1. Physical Setup

The scintillator used for this experiment is the Eljen Technologies EJ-200 plastic scintillator[2], coupled to the

[2] https://eljentechnology.com/products/plastic-scintillators/ej-200-ej-204-ej-208-ej-212

ETEL 9390B photomultiplier tube[3], with the entire assembly wrapped in an internal reflective cover and an opaque black vinyl cover. The EJ-200 scintillator is made of Polyvinyl-Toluene, which provides a very fast response time (around 2.1 ns), which we can take as the error in our time measurements. The 9390B photomultiplier has 10 dynodes, providing an amplification of 58.5 dB when powered at 1000 V. The assembly is constructed in such a way that the height of the detected peak is not dependent on position—more details are available in [11].

By wrapping the scintillator in opaque plastic, we shield the detector from most terrestrial radiation. The most common radioactive isotope in most environments is Radon, a noble gas that decays via alpha decay. Because the heavy alpha particle can be shielded by a thin layer of plastic, it will not be detected. Other radioactive decays—especially those emitting gammas—may be detectable, but should be relatively uncommon in a lab setting.

The discrimination and amplification circuitry is integrated in the photomultiplier tube, leaving us with a single BNC output whose signal is proportional to the number of electrons detected. This output is connected to a TDS-2000 oscilloscope triggered to begin a capture upon detecting a voltage above some threshold—i.e. a peak. If the incident muon was successfully stopped, there will be a second event shortly afterwards from the muon decaying, which will be resolved as a second peak on the oscilloscope[11].

2. *LabView Data Acquisition*

The oscilloscope is then connected to a PC running NI LabView through a GPIB cable. The LabView program waits until the scope is triggered by a peak before transferring the waveform over. If a peak-finding algorithm detects two distinct peaks, the time difference between the peaks is recorded in a spreadsheet file. If only a single peak is detected, the waveform is discarded.

3. *False Decays*

Although most closely-spaced peaks are due to a muon arriving in the detector and decaying, some can be caused by the arrival of two closely-spaced muons. Because the energies of incidence events and decays are not markedly different, we cannot discern these events from actual decays. Instead, since the distribution of time differences in these events will be uniform, we can consider a distribution of form

$$N = N_0 e^{-t/\tau} + B \tag{6}$$

[3] `http://et-enterprises.com/images/data_sheets/9390B.pdf`

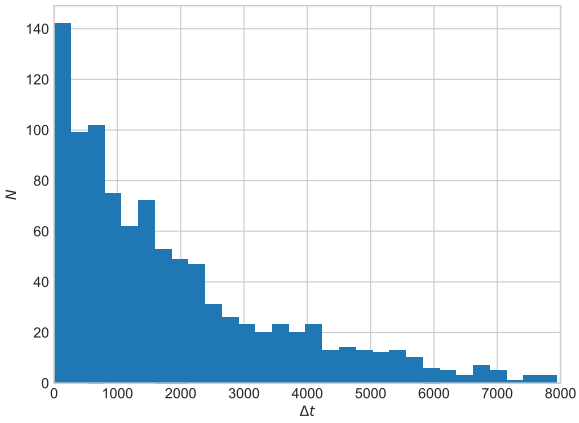

FIG. 4: A simple histogram. Note that a fixed bin width does a poor job capturing the wide range of slopes in the model.

instead of a pure exponential decay, and adjust our fit accordingly.

B. Data Grouping

After running the experiment, we will (hopefully) have a long list of Δts between incidence and decay. We can consider these to be observations of a random variable distributed according to equation 6, and attempt to estimate the parameters of the underlying distribution by fitting a curve. This is a surprisingly nuanced thing to do, especially for an exponential distribution. I will briefly discuss various methods, including their advantages and disadvantages.

1. *Simple Histogram*

The simplest approach to this sort of problem is to plot the data in a histogram and consider each bin a point, with its x-value given by its center and its y-value by its height, and fit to these points. A histogram of this kind (with data generated to resemble the experimentally collected data) is shown in figure 4. A few problems become readily apparent with this approach. The fixed bin width poorly captures the wide variation in slopes, with a blocky slope at low Δt, where the slope is steepest; and near-empty bins on the sparse right tail. This poor model of the underlying distribution affects our ability to fit a curve, increasing our uncertainty. Empty bins also present a problem during fitting, since fitting to an exponential involves taking the log of the y-value, and $\log 0$ is undefined.

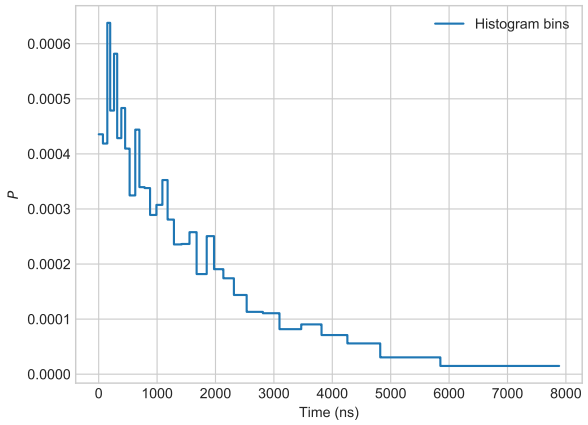

FIG. 5: A histogram with variable sized bins, over the same data as fig. 4

2. *Equiprobable Bins*

We can improve our fit by moving to variable bin widths, using narrow bins on the steep left half of the graph, and wide bins on the flat right side. A commonly used technique for this is that of equiprobable bins, where bins are sized such that each one has an approximately equal number of points. Figure 5 shows an example of this. When using these equiprobable bins, the optimum number of bins tends to be around [14]

$$\#\text{ of bins} = 2N^{2/5}.$$

Note than, when using this technique, you must tell the histogram function that you are plotting a PDF, since otherwise the histogram will be flat (for `numpy`'s `np.histogram`, passing the option `density=True` accomplishes this).

To calculate these bins, the simplest (although maybe not the fastest) algorithm involves sorting the data, before slicing it up into approximately equal batches. A reference implementation in Python (as well as other pitfalls to be aware of using this technique) is available at [15].

3. *Kernel Density Estimation*

Just as summing over a discrete random variable can be generalized to integrating over a continuous one, we can generalize the histogram into a continuous form. Instead of grouping variables into discrete bins and plotting the density of the bins, we consider each observation to be a small Gaussian (with adjustable variance), and sum up all the Gaussians to get an approximation of our data's PDF (as seen in figure 6) [16]. Figure 7 shows the density function estimate for our data.

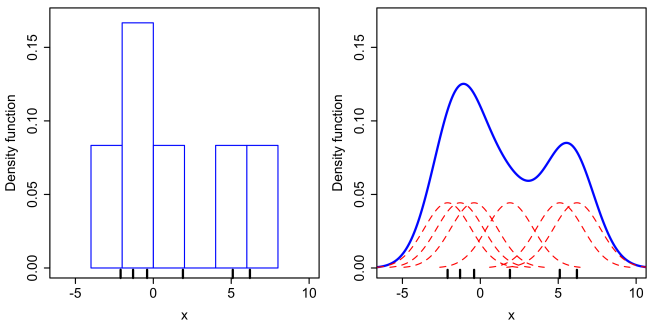

FIG. 6: This figure illustrates the relationship between a discrete histogram and a continuous KDE. Figure from `https://commons.wikimedia.org/wiki/File:Comparison_of_1D_histogram_and_KDE.png`, licensed under CC-BY-SA.

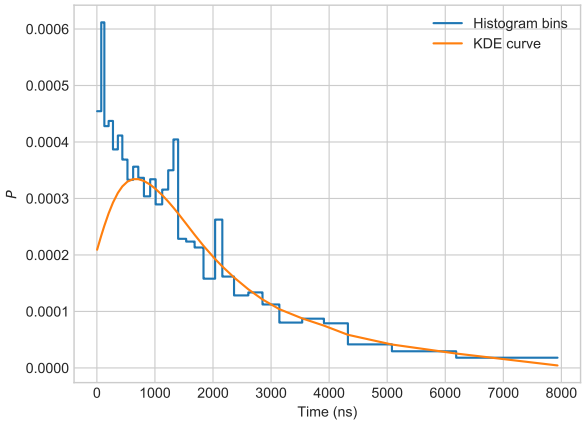

FIG. 7: The kernel density estimate, overlaid on the variable width bins from earlier.

Although it fits the data wonderfully, and would lead to a very robust analysis, there were some concerns that led to me not using this method. First, the lack of observations at $\Delta t < 80$ (since we purposefully culled these) is interpreted as the density function being 0 at these points, and leads to an unrealistically low estimate for low t. There is likely some way to specify the domain over which to estimate, but I was not able to find one[4]. Second, I am unsure how to propagate errors using this method, so any estimate of the lifetime using this method would be unrealistically precise.

[4] I believe this is because the technique is typically used to estimate two-tailed distributions, where this is not a concern. The function used here is documented at `https://docs.scipy.org/doc/scipy/reference/generated/scipy.stats.gaussian_kde.html`.

C. Curve Fitting

Once we obtain a function or collection of points approximating the distribution of times (using one of the methods described earlier), we must fit an exponential distribution to estimate the lifetime τ.

1. Simple Linear Fit

Assume we have a distribution of form

$$N(t) = N_0 e^{-\lambda t}.$$

where $\lambda = 1/\tau$. If we take the log of both sides, we get that

$$\log(N(t)) = \log(N_0) - \lambda t$$

which describes a simple linear relationship between t and $\log N$. Linear ordinary least squares (linear OLS) provides a robust, unbiased, efficient estimator for this kind of relationship, and is easy to implement and understand.

However, doing a simple linear fit to $\log N$ emphasizes small values of N, leading to a biased estimator. We can correct for this by weighting larger values of N [17] by $\sqrt{N}$. This provides the BLUE (best linear unbiased estimator) for an exponential relationship.

2. Linear Fit with Background Subtract

Recall from earlier that the distribution of our data is not purely exponential—there is also some constant component, so the distribution is actually

$$N(t) = N_0 e^{-\lambda t} + B$$

If we try to perform a simple linear fit on this data, our timescale τ will be larger than it should be, since the distribution does not converge to 0 as expected. Figure 8 shows this effect.

We can, however, easily correct for this. At a distance of $t = 5\tau$ (where $\lambda t = 5$), the exponential curve has dropped to near-0—specifically, it is 0.6% of its initial value. Most height in our fit is due to the constant portion. We can subtract this height from our PDF to eliminate most of the background. By repeating this process a few times, we can quickly converge on a truly exponential distribution [18].

3. Nonlinear Fitting

Alternatively, we can avoid the problems of weighting and background subtract by directly fitting to a nonlinear model, and estimating the parameters $N_0, \lambda,$ and B directly in

$$N(t) = N_0 e^{-\lambda t} + B$$

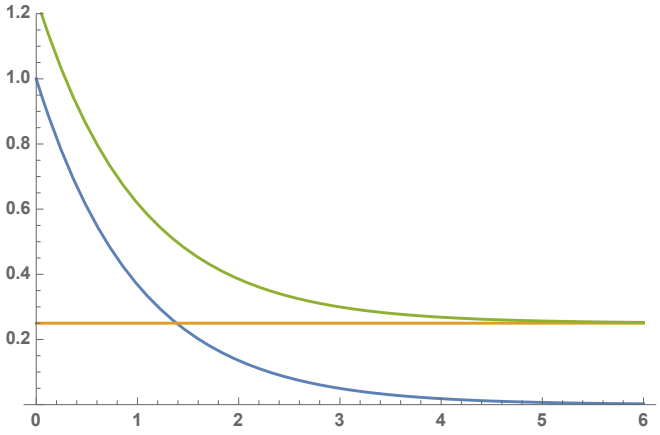

FIG. 8: The true shape of our distribution, as the sum of an exponential and constant distribution. In this example, $\lambda = 1$ and $B = 1/4$.

Because the nonlinear least squares problem has no analytic solution (unlike linear least squares), we must provide reasonably accurate starting values for the fitter to work from—such as the output from a simple linear fit. To accurately estimate the background and separate it from the exponential, we also need a well-populated long tail (going up to 5τ or so).

The other advantage of nonlinear least squares involves precision errors in calculating the log function for a linear fit. Internally, our data are stored by the computer as floating-point numbers, typically with 64 bits of precision. These numbers have three components—the sign (a single bit, which we can denote as S), the fraction (F), and the exponent (E). The number x is then given by

$$x = (-1 \cdot S) \cdot F \cdot 2^E$$

Because of this imprecision, doing arithmetic with floating point numbers introduces inaccuracies, especially if the exponents involved are drastically different. Since, as we perform our background subtraction procedure, some numbers rapidly approach 0, this has the potential to affect the accuracy of our fit when we take the log. By performing a nonlinear fit, we avoid the problem of background subtraction and floating-point imprecision.

D. Monte-Carlo Analysis of Estimators

Given a fitting routine, we want to ensure that it will actually estimate the actual parameter without bias, and that its performance improves with a larger sample size (in statistical terms, we want to ensure that it is *unbiased* and *consistent*). We can do this by generating data from a known distribution mimicking the expected experimental distribution, and analyzing that data using our fitting routine. If the estimate is close to the value used to generate the distribution, we can be confident in our estimator [19].

By repeating this process for hundreds or even thousands of generated datasets, we can examine the distribution of estimators and errors to predict the reliability of the estimator. This technique was used when coding and comparing the estimators above, to verify their performance on both perfect datasets (no deviation from the model) and datasets very similar to the experimental data.

IV. RESULTS & ANALYSIS

We allowed the experiment to run for a cumulative time of around 60 hours, spread throughout the course of a few weeks; and observed a total of 1125 muon decays. Measurements of less than 80 ns were discarded, to ensure the scintillator and photomultiplier tube had adequate time to reset between peaks. Because of the concerns with the kernel density method described above, the method of equiprobable bins was used to group the data, as seen in figure 9.

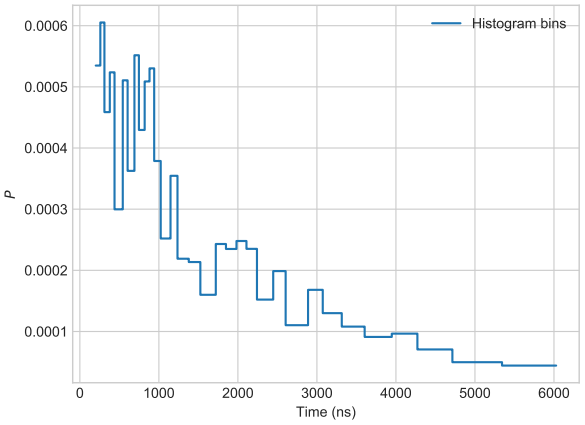

FIG. 9: The observed muon decays, grouped into equiprobable bins.

Note that we do not have any observations beyond 3τ—this is due to experimental error in configuring the oscilloscope. Due to this limitation and the relatively small sample size, we chose to use a linear fit with background subtract to estimate the lifetime of the muons. Figure 10 shows the results of this process, with an observed lifetime of $\tau_{\text{obs}} = (2058 \pm 86)$ ns

Recall from equation 4 that the expected decay time in a plastic scintillator, assuming an equal mix of μ^+ and μ^-, was (2117 ± 3) us—giving us an error of 0.68σ. We therefore have no evidence to support rejection of the null hypothesis, and the results of this experiment are in line with previous measurements of the decay time of muons in matter.

Alternatively, we can use equation 5 to estimate the ratio of μ^+ to μ^-, giving

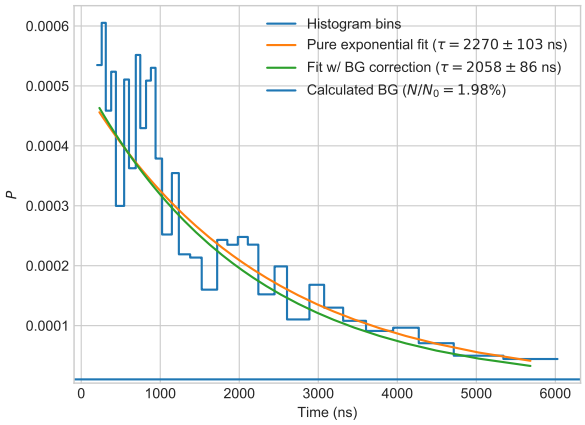

FIG. 10: The observed muon decays, and exponential fits using the background-subtract model. Background was found to be 2% of the exponential decay at $\Delta t = 0$.

$$\hat{\rho} = 0.116 \pm 0.737$$

If we take $\rho = 1$, this gives an error of 1.36σ. Since, as explained in the theory section, $\rho > 1$ with almost certainty, this indicates that our estimated time is somewhat low. Although not enough to reject the null hypothesis at a 95% level of confidence (1.96σ), it is somewhat concerning.

A. Sources of Error

I believe the dominant source of error is due to the truncated tail of the observed distribution. If we had set the oscilloscope to capture measurements beyond 3τ, it would have been possible to perform a more accurate linear fit, or even a nonlinear exponential fit.

The other source of error is likely a too-small N. If the experiment had been allowed to run longer, we would have more datapoints to fit, especially in the long tail. This would have lowered the variance in the estimator and allowed further discernment of the exponential and constant distributions.

Finally, using the kernel density estimation method to group the data would have lowered the variance of the fit. Going from a thousand observations to around 30 bins, by definition, a simplification that reduces the amount of information available. Using a kernel density estimator (appropriately set, of course, for an exponential distribution) minimizes this loss of data and lowers the variance. Although a highly biased estimate, fitting to the KDE of this data resulted in a variance of around 5 ns—far lower than the variance of 86 ns using the process described above.

I do not believe that uncertainty in the time measurements played any significant role. The scope was set to have a resolution of 2.5 ns—approximately $(1/1000)\tau$. These errors would also tend to be averaged out and minimized by the binning process. If the KDE method were used, this error could be accounted for by slightly increasing the width of the individual Gaussian kernels of each measurement.

V. CONCLUSIONS

We were successfully able to measure the lifetime of cosmic-ray muons in plastic, finding a lifetime of $\tau = (2058 \pm 86)$ ns, consistent with the accepted value of (2.117 ± 0.003) µs. However, this low estimate of the lifetime gave an estimate of ρ, the ratio of positive muons to negative muons, of 0.116 ± 0.737—which is concerning, since there is no physical way for $\rho < 1$ unless more μ^- than μ^+ are created in cosmic ray interactions with matter.

The bulk of the error is due to experimental error in configuring the oscilloscope. When configuring the experiment, we did not allow decay times greater than 6000 ns—a lifetime of only 3τ. Without this long tail to assist in the fit, the variance of our estimator is larger than it would otherwise be, and our background subtraction routine is less precise. If we had fully captured the long tail, we would have been able to produce a more precise estimate of τ, including using the more robust nonlinear least squares estimation method.

A. Future Work

Repeating this experiment with a larger, more complete dataset would be worthwhile. All of the analytical techniques discussed in §III produce consistent estimators, which converge on the actual value as the number of observations increases. Running the apparatus for a period of weeks or months, or using data from multiple detectors running simultaneously, would yield tens of thousands of observations and lower the variance in our estimate.

Using the kernel density estimation method, we could also improve our estimate of τ. Creating a histogram is an inherently lossy process, and increases the variance in our fit. However, the documentation I found did not specify how to use this method for the exponential distribution, and I was not able to successfully perform this analysis.

The analytic methods detailed in this paper are also broadly applicable to studying exponential decays in general, including radioactive decay and the decay of other particles. The techniques described here may be useful in nuclear physics, or even classical mechanics—anywhere we may be dealing with a population of unstable particles.

ACKNOWLEDGMENTS

I would like to thank my lab partner Miles Cohen, for his assistance in collecting data and in refining my data analysis. I would also like to thank John Essick, for answering endless questions, and for writing an unrivaled LabView guide.

[1] M. Tanabashi *et al.* (Particle Data Group), Phys. Rev. D **98**, 030001 (2018).
[2] S. H. Neddermeyer and C. D. Anderson, Physical Review **51**, 884 (1937).
[3] J. C. Street and E. C. Stevenson, Phys. Rev. **52**, 1003 (1937).
[4] K. C. Koenigsmann, (1973), 10.2172/4328412.
[5] M. Ackermann *et al.*, Science **339**, 807 (2013), arXiv:1302.3307 [astro-ph.HE].
[6] J. Abraham *et al.* (2009).
[7] D. Maoz, *Astrophysics in a Nutshell*, In a Nutshell (Princeton University Press, 2007).
[8] M. Wolverton, Scientific American **297**, 26 (2007).
[9] R. R. R. Staff, "Reed research reactor training manual 2017-18," (2017), email thmalthou@reed.edu for a copy.
[10] G. Knoll, *Radiation Detection and Measurement* (John Wiley & Sons, 2010).
[11] N. D. Woo, *A Large-Volume Scintillation Detector for the Study of Cosmic-Ray Muons*, Thesis, Reed College, 3203 SE Woodstock Blvd (2015).
[12] B. Rossi, *High-energy particles.*, 2nd ed. (Prentice-Hall, New York,, 1956).
[13] R. A. Reiter, T. A. Romanowski, R. B. Sutton, and B. G. Chidley, Phys. Rev. Lett. **5**, 22 (1960).
[14] NIST, "Chi-square goodness of fit test," .
[15] farenorth, "Matplotlib: How to make a histogram with bins of equal area?" .
[16] J. VanderPlas, *Python Data Science Handbook* (O'Reilly Media, 2016).
[17] S. D. Foss, Biometrics **26**, 815 (1970).
[18] T. Coan and J. Ye, TeachSpin, Inc..
[19] R. Hill, W. Griffiths, and G. Lim, *Principles of Econometrics* (Wiley, 2007).